Available online at www.sciencedirect.com

SciVerse ScienceDirect

Ceramics International 38 (2012) 5979–5986

CERAMICS INTERNATIONAL

www.elsevier.com/locate/ceramint

Microstructural evolution and contact-mechanical properties of SiC ceramics prepared colloidally with low additive content

O. Borrero-López, A.L. Ortiz *, E. Ciudad, F. Rodríguez-Rojas, F. Guiberteau

Departamento de Ingeniería Mecánica, Energética y de los Materiales, Universidad de Extremadura, Badajoz, Spain

Received 12 March 2012; accepted 17 April 2012
Available online 24 April 2012

Abstract

The microstructural evolution and contact-mechanical properties of liquid-phase sintered (LPS) SiC ceramics processed colloidally with low loads of sintering additives was investigated as a function of the sintering duration, and was compared with the case of their counterparts processed conventionally. The two processing routes differ in the preparation of the powder batch, which in the colloidal method is done by covering the SiC particles with an oxide nano-film synthesized by the sol–gel method, whereas in the conventional method it is done by mixing mechanically the SiC powder with the oxide powders. It was found that the colloidal processing route offers clear benefits in terms of densification and contact-mechanical properties (stiffness, hardness, and damage and wear resistances) over the conventional processing route when the sintering times are short, but not when the sintering times are moderate or prolonged. Furthermore, no differences were found in the microstructural evolution with the sintering duration between the two types of ceramics. Based on the results, it is proposed that the more sophisticated colloidal processing route is certainly the appropriate choice for short sintering times, whereas in other cases its use would be justified if the goal is to incorporate into the microstructure new homogeneous multi-component oxide additives with tailored stoichiometry.

Keywords: D. SiC; Pressureless sintering; Colloidal processing; Contact-mechanical properties

1. Introduction

Silicon carbide (SiC) is one of the most important non-oxide structural ceramics due to its excellent combination of physical and chemical properties, namely, high strength, stiffness, hardness, and wear resistance, as well as chemical stability, oxidation resistance, and high melting point [1–5]. Moreover, SiC ceramics with near-net complex shapes can be processed pressureless at moderate temperatures—i.e., at relatively low cost—via liquid-phase sintering by including suitable combinations of sintering additives, thus resulting in two-phase materials with hard SiC grains and a softer secondary phase [6]. Most commonly, a combination of Al_2O_3 and Y_2O_3 additives in a 5:3 molar ratio is employed to obtain a crystalline $Y_3Al_5O_{12}$ (YAG) secondary phase [7], although Al_2O_3 has also been combined with other rare-earth oxides to form different crystalline garnets [8–10].

While the secondary phase can be beneficial in order to improve some room-temperature mechanical properties of liquid-phase-sintered SiC (LPS SiC)—especially the fracture toughness due to the activation of crack bridging mechanisms in the wake of the crack tip [2,6,8]—other properties can be impaired by it. In particular, it has been shown that increasing the content of the softer secondary phase results in the decrease of contact-mechanical properties such as elastic modulus, hardness, and wear resistance [6]. Moreover, the secondary phase has been found to deteriorate with prolonged sintering, also contributing to property degradation [11].

Based on the above, one of the processing guidelines which has been proposed to fabricate LPS SiC ceramics with engineered mechanical properties is to use low amounts of sintering additives together with short sintering times [12,13]. However, under such circumstances complete densification is difficult to achieve pressureless if one starts from the conventional mechanical mixture of powders (SiC plus the additives) because the liquid phase formed from particulate additives does not distribute appropriately in the microstructure. To solve that problem, a colloidal processing route has

* Corresponding author. Tel.: +34 924289600x86726; fax: +34 924289601.
E-mail addresses: alortiz@materiales.unex.es, alortiz@unex.es (A.L. Ortiz).

0272-8842/$36.00
http://dx.doi.org/10.1016/j.ceramint.2012.04.051

recently been developed in which a precursor sol–gel solution is deposited onto the individual SiC particles to achieve the uniform distribution of the sintering additives in the microstructure required for the obtaining of full-dense LPS SiC ceramics with low additive content (3.6 vol.%) at short sintering times (1 h) [14]. As a result of the improved densification, the LPS SiC ceramic prepared colloidally has greater sliding-wear resistance than its counterpart prepared conventionally, providing evidence that this new route is indeed advantageous for short sintering times.

Given that the colloidal processing route appears to offer the possibility of overcoming some fundamental limitations of LPS SiC ceramics, it seems timely to examine in detail various important aspects of these new LPS SiC ceramics not yet investigated. In particular, three issues that require special research attention are: (i) the elucidation of the microstructural evolution with the duration of sintering, (ii) the evaluation of other relevant contact-mechanical properties apart from wear, and (iii) the correlation between the sintering duration and the contact-mechanical properties. This was indeed the objective of the present work which was aimed at exploring these three pending issues of colloidally prepared LPS SiC ceramics as well as at comparing the microstructural development and the contact-mechanical properties of the colloidal and conventional LPS SiC ceramics fabricated for different sintering times (1–7 h) because this comparison is also essential for elucidating the true potential of the colloidal processing route. The interest of the present work is that it may assist in selecting the processing strategy which is best suited for the fabrication of low-cost LPS SiC ceramics with prescribed contact-mechanical properties.

2. Experimental procedure

2.1. Processing

Two powder batches were prepared, one by colloidal processing and the other by conventional processing, specifically designed to yield LPS ceramics with 96.4 vol.% SiC and 3.6 vol.% YAG. In both cases, the same commercially available submicrometre α-SiC (UF-15, H.C. Starck) powder was used, but the YAG phase was obtained and introduced in different manners. In the colloidal processing route, a ceramic suspension was prepared by immersing 95 g of the SiC powder in a custom-made YAG precursor sol–gel solution, followed by vigorous agitation until complete dispersion and then total drying, first on a hot plate while being stirred and then in an oven at 100 °C. The YAG sol–gel solution was synthesized from another two sol–gel solutions, one rich in Al and the other in Y, as follows. The Al-rich solution was prepared by mixing 11.4 cm^3 of aluminium s-butoxide (13044, Alfa Aesar) in 115 cm^3 of 2-propanol (141090, Panreac, Spain) plus 5.7 cm^3 of nitric acid 69% (141037, Panreac) until complete solution, and then adding 1.7 cm^3 of distilled water with stirring for the corresponding hydrolysis. The Y-rich solution was prepared similarly from 9 g of yttrium acetate (14565, Alfa Aesar), 115 cm^3 of 2-propanol, and 6.7 cm^3 of nitric acid, but without the addition of water because the alkoxide contains enough water for the hydrolysis. The two sol–gel solutions were then mixed together until complete homogenization.

In the conventional processing route, 95 g of the SiC powder was mechanically mixed with 2.15 g of Al_2O_3 powder (AKP-30, Sumitomo Chemical Company) and 2.85 g of Y_2O_3 (Fine-Grade, H.C. Starck) powder until complete homogenization using the typical procedure of intimate blending via wet-ball-milling in ethanol. The resulting ceramic slurry was hot-plate and then oven dried as in the colloidal processing route.

The powders prepared colloidally and conventionally were compacted into several disks by uniaxial pressing (C, Carver Inc.) at 50 MPa, followed by isostatic pressing (CP360, American Isostatic Press) at 350 MPa. Each compact was then embedded individually in loose powder beds composed of 90 wt.% SiC (600 grit; Crystolon, Norton Co.) and 10 wt.% Al_2O_3 (15 μm, Buehler) inside graphite crucibles, and was pressureless sintered in a graphite furnace (1000-3560-FP20, Thermal Technology Inc.) at 1950 °C under a flowing Ar-gas atmosphere of 99.999% purity for times between 1 h and 7 h to span from short to long sintering treatments. The resulting sintered SiC ceramics, henceforth referred to simply as colloidal or conventional ceramics, were all cleaned and ground down 1 mm to remove the adhered layer of powder bed. Finally, the surface was polished to a 1-μm finish using routine ceramographic methods.

2.2. Characterization

The density of all colloidal and conventional LPS SiC ceramics was measured using the Archimedes method with distilled water as the immersion medium. The microstructures were revealed by plasma etching these polished surfaces with CF_4 + 4% O_2 gas for 2 h, and then observed under scanning electron microscopy (SEM; S-3600N, Hitachi). The microstructural observations were done with secondary electrons, at 20 kV accelerating voltage. The average size and shape of the SiC grains in each material was quantified by image analysis (AnalySIS, Olympus Soft Imaging Solutions GmbH), on the basis of at least 300 grains from different SEM micrographs taken randomly.

2.3. Evaluation of contact-mechanical properties

2.3.1. Vickers indentation

Cross-sections of all sintered materials were also polished to a 1-μm finish, and were subjected to Vickers-indentation tests to evaluate the hardness and toughness. The tests were performed using a hardness tester (MV-1, Matsuzawa) equipped with a Vickers diamond pyramid, under the following conditions: load peak of 98 N, load application rate of 40 μm/s, and dwell time of 20 s. Ten separate indentations were done for each material. Subsequently, the tested surface was gold-coated for the measurement of the length of the diagonal of the residual impression and of the total length of the surface trace of the radial cracks under optical microscopy (Epiphot 300, Nikon). The hardness and toughness were computed using standard formulae [15,16].

2.3.2. Hertz indentation

The polished cross-sections of all sintered materials were also subjected to Hertzian indentation tests. These contact-mechanical tests were performed with the surfaces previously gold-coated, using a universal testing machine (5535, Instron) at a constant cross-head speed of 0.05 mm/min and under the following conditions: load range between 15 and 1000 N, and WC spherical indenters of radius 7.94 to 1.58 mm. The contact radius of each residual impression was then measured under the optical microscope, and was used to construct the indentation stress–strain curves. The elastic modulus of each sintered material was determined from the linear stretch of its indentation stress–strain curve using a standard formula [17,18].

2.3.3. Wear

Three polished disks were core-drilled from each of the two types of ceramics with selected sintering times (1 h and 7 h), to be used for wear testing. The wear tests were performed in a tribometer (High-Performance Multi-Specimen, Falex Corp.) configured in the ball-on-three-disks geometry, under the following conditions: bearing-grade Si_3N_4 ball (NBD 200, Cerbec) of radius 6.35 mm, total lubrication with paraffin oil, contact load on each disk of 80 N, rotation speed of 100 rpm, and sliding time between 5 s and 500 min. The wear curves were constructed by repeating successive steps of interrupting the test at predesigned time intervals to measure the diameter of the wear scar on each disk (two orthogonal measurements per disk, 3 disks per ceramic) and then putting the bearing assembly back in the tribometer for further wear.

3. Results and discussion

Fig. 1 shows representative SEM images of the microstructure of the colloidal and conventional LPS SiC ceramics resulting from the sintering of the shorter (i.e., 1 h) and longer (i.e., 7 h) durations. Clearly, the microstructure consists always of equiaxed SiC grains with an oxide secondary phase located mostly at the triple junctions of the grain structure. Nevertheless, the detailed comparison of the SEM images in Fig. 1A and B reveals that the microstructure of the colloidal ceramic is more homogeneous than that of the conventional ceramic when the sintering time is short. In particular, the colloidal ceramic exhibits a better distribution of the secondary phase, and also a lesser population of defects or porous regions which in addition are smaller (∼0.2 μm vs. ∼1 μm). Indeed, the measurements of density by the Archimedes method confirmed that the colloidal ceramic is full-dense within the experimental error

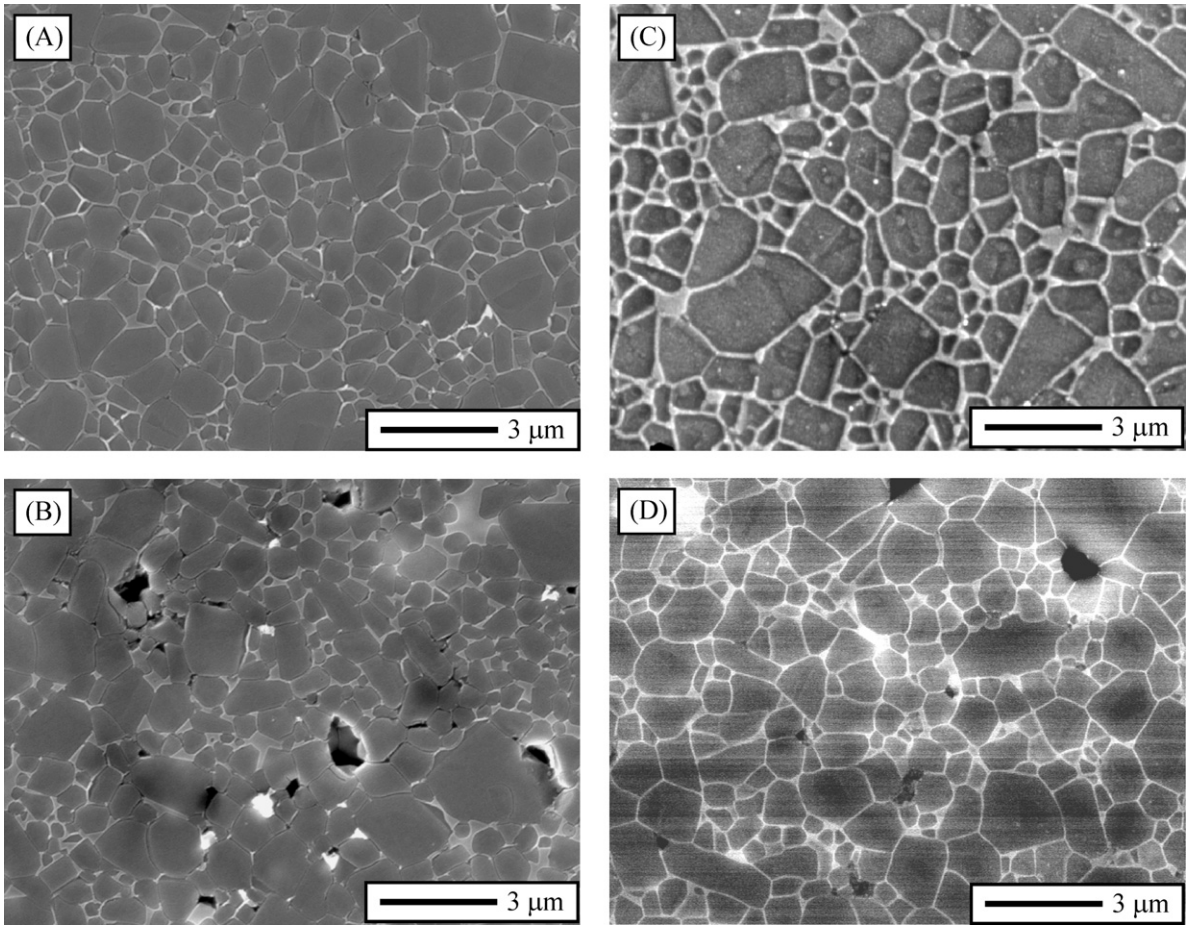

Fig. 1. SEM micrographs of the polished and plasma-etched cross-sections of the LPS SiC ceramics prepared (A) colloidally with 1-h sintering, (B) conventionally with 1-h sintering, (C) colloidally with 7-h sintering, and (D) conventionally with 7-h sintering.

(i.e., 3.261 g/cm^3 density), while the conventional ceramic has ∼5% porosity (i.e., 3.098 g/cm^3 density). This poorer densification achieved by the conventional processing route is because the particulate dispersion of the sparse sintering additives (i.e., 3.6 vol.%) between the SiC grains induces the local formation of a discontinuous liquid phase, and the short sintering times are insufficient to redistribute it homogeneously. That at short sintering times a full-dense, homogeneous ceramic is obtained by the colloidal processing route is doubtless the result of the much better dispersion of the sintering additives achieved by this method, in which the precursor additives continuously coat all the SiC particles thus inducing the formation of a continuous liquid phase. The comparison of the SEM images in Fig. 1C and D indicates, however, that the scenario changes when the sintering time is sufficiently long, with both the colloidal and the conventional processing routes resulting in homogeneous, pore-free microstructures. Indeed, the density measurement by the Archimedes method performed on the two types of ceramics with 3 h of sintering revealed that there were already no differences (i.e., ∼3.261 g/cm^3). It can thus be concluded that sintering beyond 1 h is the condition required for the liquid phase generated from low contents of particulate sintering additives to redistribute homogeneously. Therefore, the clearest advantage of the colloidal processing route over the conventional one is that it is exempt from this condition, and the shortening of the sintering time has important implications with a view to commercial mass production. As will be discussed below, this does not mean that colloidal processing does not also offer some advantages for prolonged sintering treatments, although clearly not in terms of densification.

Fig. 2 compares the evolution of size and morphology of the SiC grains with the sintering time for the colloidal and conventional LPS SiC ceramics. It can be observed that the average size of the SiC grains depends on the sintering duration, but not on the processing route. The increase of the grain size in the two types of ceramics from ∼0.6 μm at 1 h of sintering to

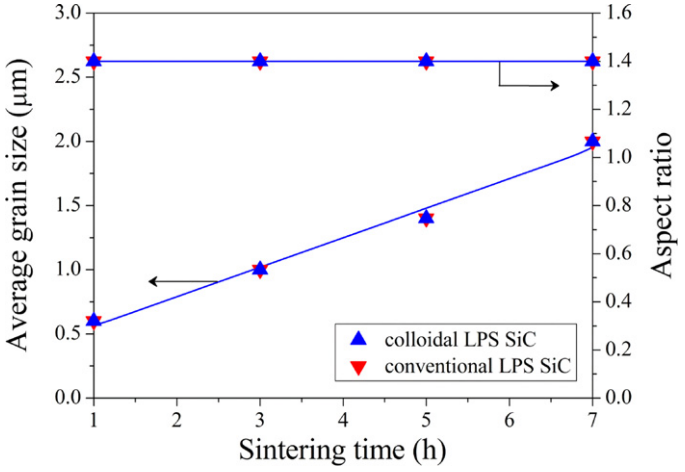

Fig. 2. Microstructural evolution as a function of the sintering time for the colloidal and conventional LPS SiC ceramics. Triangles are the experimental data, and solid lines are to guide the eye. The error bars are smaller than the symbol size.

∼2 μm at 7 h of sintering is due simply to the microstructure coarsening by solution-reprecipitation (Ostwald ripening) that occurs during the continued liquid-phase sintering [19,20]. After 1 h of sintering the grain size has changed very little (in particular, it has grown only by ∼0.1 μm) with respect to the starting condition of ∼0.5 μm, and this marginal grain growth is the reason for the observed similarity of the colloidal and the conventional ceramics despite the better distribution of liquid phase in the former. Furthermore, neither past 1 h of sintering does the grain size depend on the processing route because both routes achieve a homogeneous distribution of the liquid phase. With respect to the morphology of the SiC grains, in Fig. 2 one observes that they are equiaxed with an aspect ratio of 1.4, regardless of the processing route and of the sintering duration. This finding is consistent with a previous study that has demonstrated that this aspect ratio is indeed the equilibrium shape of the α-SiC grains in LPS SiC ceramics [19]. With this information it can be concluded that the microstructural development of the LPS SiC ceramic is not conditioned by the processing route (i.e., colloidal or conventional method) chosen to disperse the sintering additives in the microstructure.

Fig. 3 compares the Hertzian indentation stress–strain curves measured for the colloidal and conventional LPS SiC ceramics with 1 and 7 h of sintering. It is evident in Fig. 3 that the shape of the Hertzian curves is the same in all cases, with a first linear stretch at low contact pressures that reflects the elastic deformation regime, followed by a second nonlinear stretch at intermediate and high contact pressures that corresponds to the quasiplastic deformation regime. Moreover, it can also be observed in Fig. 3 that a certain divergence appears between the colloidal and conventional LPS SiC ceramics with 1-h sintering, especially in the quasiplastic deformation regime but also in the elastic deformation regime. For the rest of the sintering times (i.e., 3–7 h), the Hertzian curves are independent of the processing route. Both observations are consistent with the fact that the response to the Hertzian indentation depends on average microstructural characteristics. Thus, the difference in the Hertzian response observed at 1 h of sintering is due to the 5% difference in porosity that makes slightly higher stresses being required to attain the same strains in the colloidal, full-dense ceramic, whereas the absence of differences in response to the Hertzian contact above 1 h of sintering reflects the microstructural similarity of the two types of ceramics. Consistently with these observations, the elastic modulus measurements shown in Fig. 4 confirmed the existence of a small difference between the two types of ceramic with 1-h sintering, but not between the ceramics with more prolonged sintering (i.e., 3, 5 or 7 h).

Larger differences arise when the Hertzian response of the ceramics sintered at different times are compared. In particular, it can be seen in Fig. 4 that the elastic modulus decreases with increasing sintering duration, as is also the case with the contact pressure required to attain a given deformation in the quasiplastic regime (compare Fig. 3A and B). These trends are due to the progressive degradation that the secondary phase undergoes with the continued exposure to the high temperatures (1950 °C in the present case) [11]. The degradation of the

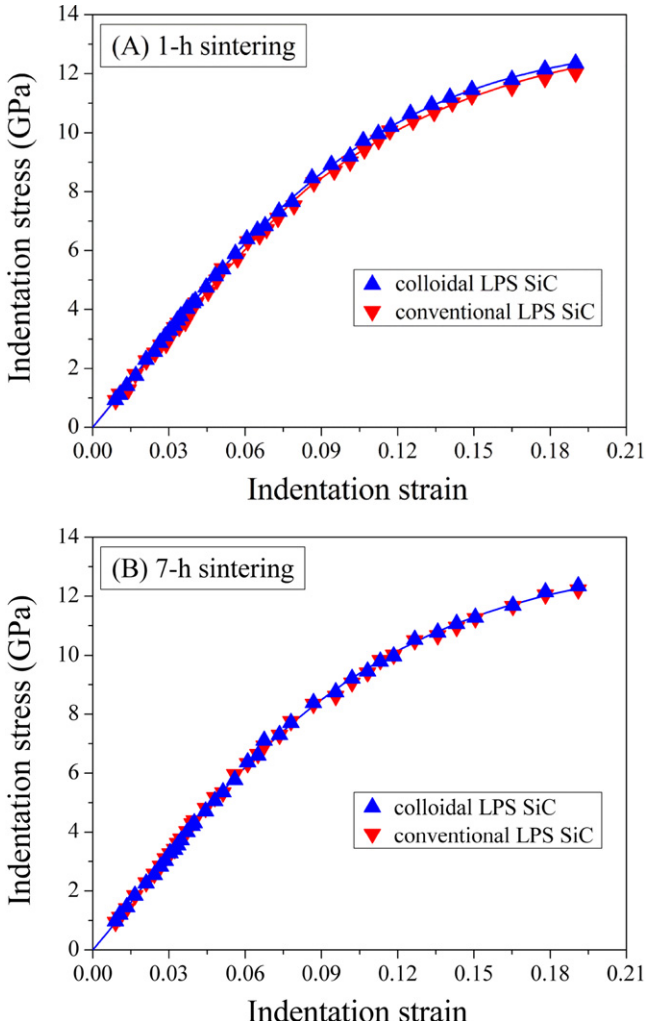

Fig. 3. Hertzian indentation stress–strain curves of the colloidal and conventional LPS SiC ceramics with (A) 1-h sintering and (B) 7-h sintering. Triangles are the experimental data, and solid curves are to guide the eye. The error bars are smaller than the symbol size.

secondary phase is a well-known fact, and is indeed the reason why LPS SiC ceramics are typically sintered within powder beds [21] so as to prevent this degradation in as far as possible by forming an excess of gas pressure rich in the metal oxides. Consistently with this degradation, it can be seen in Fig. 5 that the hardness of the colloidal and conventional LPS SiC ceramics decreases by ∼22% as the sintering duration increases from 1 h to 7 h, with the fall being more pronounced from 3 h of sintering. It can also be seen that the hardness of the conventional LPS SiC ceramic did not change much between 1 h and 3 h of sintering, which is because the effect of the secondary phase degradation is partially counterbalanced by the increase in densification (from 95% density to full-dense). Furthermore, comparison of the hardness values in Fig. 5 reveals that, except for the small difference in hardness at 1 h of sintering, the colloidal and conventional LPS SiC ceramics are equally hard. Clearly, the slightly greater hardness of the colloidal ceramic at 1 h of sintering is not due to a greater hardness of the SiC grains or of the secondary phase, but simply to the ∼5% residual porosity in the conventional ceramic.

The SEM examination of the propagation of the cracks generated in the Vickers indentations revealed that all colloidal and conventional LPS SiC ceramics, regardless of the sintering time, fractured intergranularly. This is consistent with the notion that LPS SiC ceramics possess weak interfaces as a result of the residual stresses induced by the thermal expansion mismatch between the SiC grains and the secondary phase [2,22,23], and are therefore not expected to be conditioned by the way in which the sintering additives are introduced. Fig. 6 shows the evolution of the fracture toughness with the sintering duration. It can be observed that the fracture toughness is independent of the processing route, with the exception of the 1-h sintering for which the conventional ceramic appears to be slightly tougher. This small difference is, however, most likely an artefact associated with the ∼5% residual porosity which helps to dissipate part of the Vickers indentation energy in

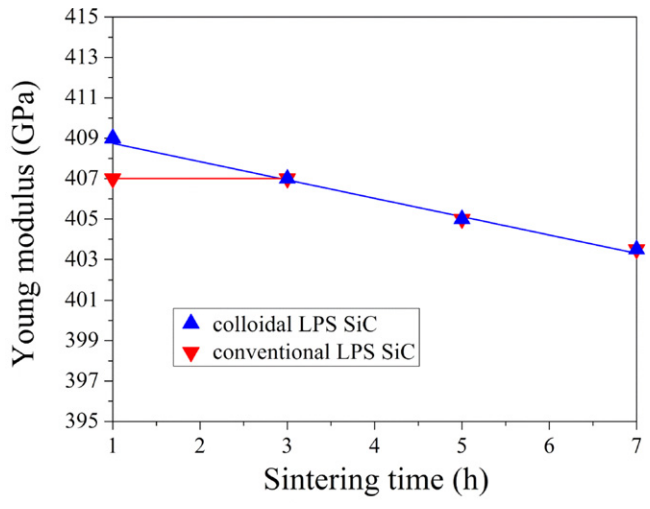

Fig. 4. Elastic modulus of the colloidal and conventional LPS SiC ceramics as a function of the sintering time. Triangles are the experimental data, and solid lines are to guide the eye. The error bars are smaller than the symbol size.

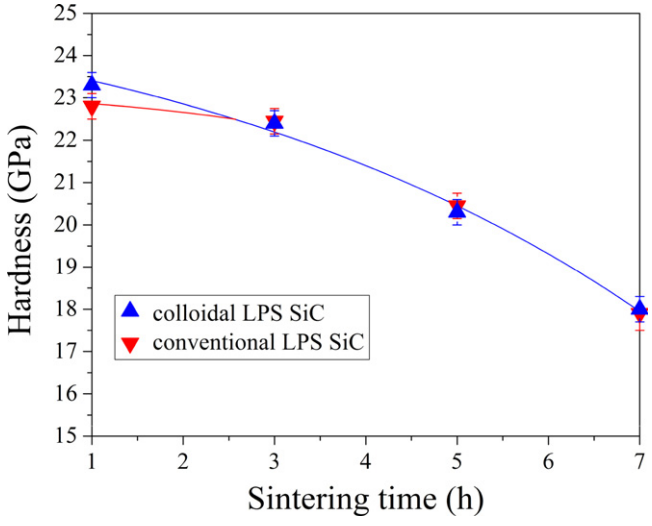

Fig. 5. Vickers-indentation hardness of the colloidal and conventional LPS SiC ceramics as a function of the sintering time. Triangles are the experimental data, and solid curves are to guide the eye.

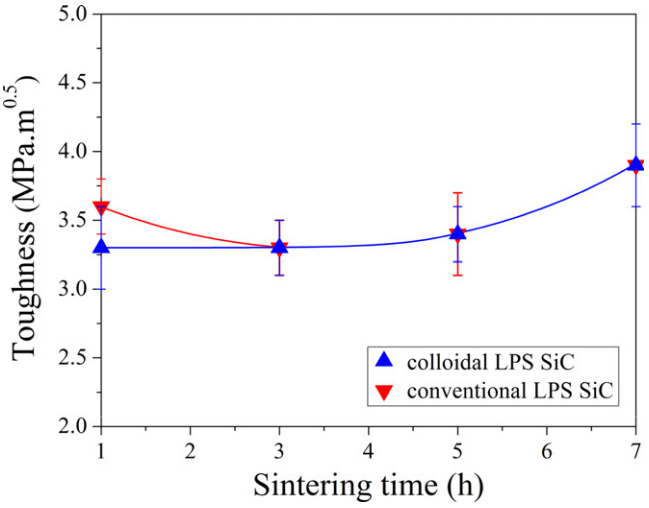

Fig. 6. Vickers-indentation toughness of the colloidal and conventional LPS SiC ceramics as a function of the sintering time. Triangles are the experimental data, and solid curves are to guide the eye.

densification, leaving less elastic energy available to drive crack propagation compared to the full-dense colloidal ceramic. It can also be seen in Fig. 6 that the fracture toughness of the colloidal and conventional LPS SiC ceramics increases by ∼18% with increasing sintering time from 1 h to 7 h. Clearly, this trend is due to the microstructure coarsening, since the larger grains are more effective in crack-wake-bridging toughening, the mechanism active in the LPS SiC ceramics [2,6,8,22].

Fig. 7 shows the sliding-wear curves of the colloidal and conventional LPS SiC ceramics with 1 h and 7 h of sintering. The comparison between these wear curves reveals three points of interest. (i) They are of the same shape as the wear curves typical of other polycrystalline ceramics, with an initial stretch that corresponds to the mild wear regime followed by a second stretch that corresponds to the severe wear regime. (ii) For the short 1-h sintering (Fig. 7A) the colloidal ceramic is more resistant to wear than the conventional ceramic, since the former enters the severe wear regime 2.14 times later than the latter (i.e., 150 vs. 70 min), with both ceramics otherwise having similar rates of mild (14.5 ± 1 μm/log *t*) and severe wear (283.5 ± 9 μm/log *t*). And (iii), for the prolonged 7-h sintering (Fig. 6B), the conventional and colloidal ceramics are equally resistant to wear, with the same rates of mild (57 ± 3 μm/log *t*) and severe (272 ± 17 μm/log *t*) wear and the same transition time between wear regimes (135 min). In order to explain the wear results, it is sufficient to consider the hardness and toughness values of the colloidal and conventional ceramics, and the SEM microstructural observations. In particular, the two types of ceramics do not differ in their mild-wear rates at 1 h and 7 h of sintering simply because these rates are dictated by the rates of accumulation of plastic-deformation damage, and the hardness of the SiC grains and secondary phase is the same in both ceramics. Furthermore, the marked increase in the mild-wear rate in both ceramics with increasing sintering time from 1 h to 7 h is due to the pronounced decrease in hardness resulting from the degradation of the secondary phase upon prolonged sintering. Regarding the

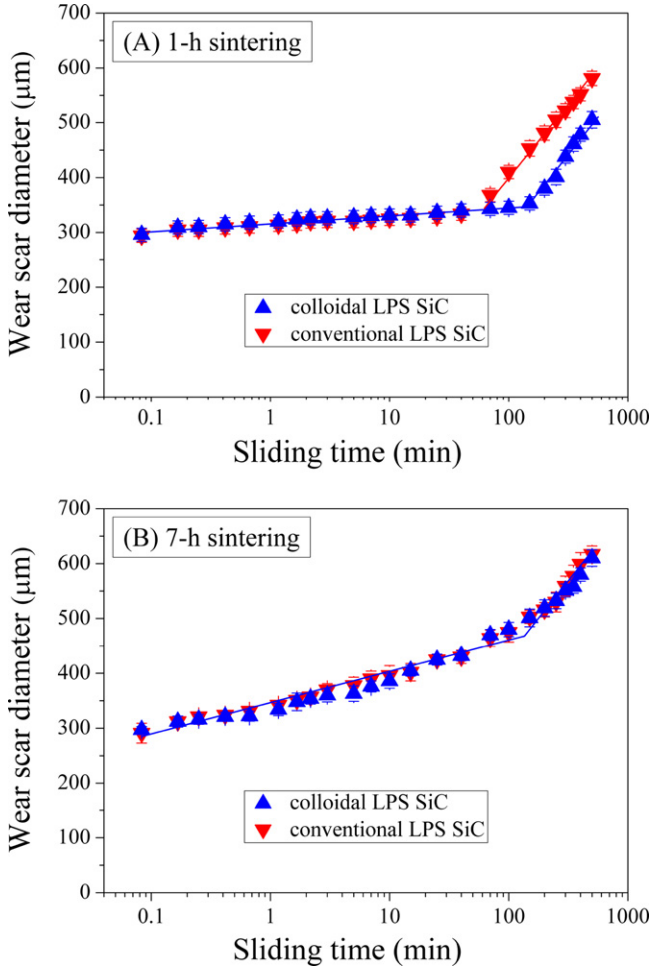

Fig. 7. Sliding-wear curves of the colloidal and conventional LPS SiC ceramics with (A) 1-h sintering and (B) 7-h sintering. Triangles are the experimental data, and solid lines are to guide the eye.

transition from mild to severe wear, this occurs when at a certain sliding time the time-dependent stress intensity factor acting on pre-existing defects under the wear contact reaches the grain-boundary toughness. Theoretically, an inverse relationship has been established between the wear-stage transition time and the average defect size [24]. Therefore, the significant delay in the wear-stage transition observed in the colloidal ceramic with 1 h of sintering is due to its smaller microstructural defects compared with the conventional ceramic. At 7 h of sintering, the similar wear-stage transition times simply reflect that the colloidal and conventional processing routes lead to the same defect population for sintering times beyond 1 h. It is also interesting to note that while the transition time in the colloidal ceramic shortens with increasing sintering duration from 1 h to 7 h, in the conventional ceramics, on the contrary, the transition time lengthens. These trends can be interpreted by taking into account that the mild-wear rate increased with the sintering time in the two ceramics, but the average size of the microstructural defects only decreased notably in the conventional ceramic because the defects in the colloidal ceramic were already as small as ∼0.2 μm at 1 h of sintering. Finally, the two types of ceramics do not differ in their severe-wear rates at 1 h and 7-h of sintering

simply because these rates depend mostly on the severity of third-body abrasion (i.e., the wear debris trapped under the contact acting as abrasive particles once grain pullout by intergranular fracture has occurred), and the abrasion factor [25] is nearly the same. The minor decrease in the severe-wear rate in both ceramics with increasing sintering time from 1 h to 7 h is likely due to the combination of the lesser fracture induced by the greater toughness and the lower hardness of the abrasive particles because of the degradation of the secondary phase.

The set of results obtained in this study reveals that the colloidal processing route is especially useful in comparison with the conventional processing route for the fabrication of low-cost LPS SiC ceramics with low additive contents when the sintering time is short. Thus, the introduction of the small amount of sintering additives by the deposition of a thin sol–gel layer on the surface of the SiC particles instead of by the typical mechanical dispersion not only allows the ceramics obtained to be full-dense, but also to have better contact-mechanical properties. The greater stiffness, hardness, and wear resistance, together with the similar toughness, are a clear demonstration of the benefits of using the colloidal processing route. Furthermore, although this aspect was not investigated in the present study, it is reasonable to expect that the colloidal processing route will also markedly enhance the strength of the LPS SiC ceramics because this magnitude scales inversely with the square root of the largest flaw size, which is about 5-times smaller in the colloidal ceramic. The present results also suggest that, in principle, for prolonged sintering times it would suffice to use the conventional processing route because, while simpler than the colloidal processing route, it leads to LPS SiC ceramics with identical microstructure (grain size and shape, as well as secondary phase distribution) and contact-mechanical properties. Having said that, it is also important to mention however that the colloidal processing route could still offer some benefits for long sintering times because it enables a better compositional design that is difficult to achieve with the conventional processing route. In particular, the ''atomistic'' mixing of the various metals in the oxide network of the nano-film deposited on the surface of the SiC particles that has been synthesized by the sol–gel method could provide an unprecedented opportunity for engineering the properties of the LPS SiC ceramics thanks to the incorporation of new homogeneous multi-component oxide additives with tailored stoichiometry.

4. Conclusions

We have studied the effect of the sintering time (1–7 h) on the microstructural evolution and contact-mechanical properties of LPS SiC ceramics prepared colloidally with the aid of sol–gel oxide solutions, and compared them with the case of those prepared conventionally from mechanically mixed powders. The results allow the following conclusions to be drawn:

1. The processing colloidal route is clearly superior to the conventional one when the sintering time is short. Thus, the ceramic prepared colloidally not only is denser than its conventional counterpart, but is also stiffer, harder, more contact-damage resistant, and more wear resistant. All these benefits emanate from the better dispersion of the sintering additives in the powder batch achieved by this method, which induces the homogeneous formation and distribution of liquid phase during sintering. Consequently, the colloidal processing route should be the reference choice for the fabrication of LPS SiC ceramics using short sintering times.
2. The microstructural development of LPS SiC ceramics does not depend on the processing route chosen to introduce the oxide sintering additives, which does not affect the coarsening by solution–diffusion–reprecipitation.
3. In terms of enhanced densification or contact-mechanical properties, the processing colloidal route does not offer benefits over the conventional one when the sintering times are moderate or prolonged. Since the powder batch preparation is simpler in the conventional processing route, its choice is therefore recommended unless the goal is to incorporate into the microstructure new homogeneous multi-component oxide additives with tailored stoichiometry, in which case the appropriate choice is the more sophisticated colloidal processing route.

Acknowledgements

The authors thank Drs. R. Caruso (CONICET-UNR, Argentina) and A. Díaz-Parralejo (University of Extremadura, Spain) for assistance with the preparation of the sol–gel solution. This work was supported by the Ministerio de Ciencia y Tecnología (Government of Spain) and FEDER funds under Grant No. MAT 2010-16848.

References

[1] G.W. Meetham, M.H. van de Voorde, Materials for High Temperature Engineering Applications, Springer, New York, 2000.
[2] N.P. Padture, In situ-toughened silicon carbide, Journal of the American Ceramic Society 77 (1994) 519–523.
[3] K.-H.Z. Gahr, R. Blattner, D.-H. Hwang, K. Pöhlmann, Micro- and macro-tribological properties of SiC ceramics in sliding contact, Wear 250 (2001) 299–310.
[4] L.S. Sigl, Thermal conductivity of liquid phase sintered silicon carbide, Journal of the European Ceramic Society 23 (2003) 1115–1122.
[5] M.E. Schlesinger, Melting points, crystallographic transformation and thermodynamic values, in: S.J. Schneider (Ed.), Engineered Materials Handbook, vol. 4, Jr. ASM International, 1991, pp. 883–891.
[6] O. Borrero-López, A.L. Ortiz, F. Guiberteau, N.P. Padture, Effect of liquid-phase content on the contact-mechanical properties of liquid-phase-sintered alpha-SiC, Journal of the European Ceramic Society 27 (2007) 2521–2527.
[7] A.L. Ortiz, F.L. Cumbrera, F. Sánchez-Bajo, F. Guiberteau, H. Xu, N.P. Padture, Quantitative phase-composition analysis of liquid-phase-sintered silicon carbide using the Rietveld method, Journal of the American Ceramic Society 83 (2000) 2282–2286.
[8] S.G. Lee, Y.W. Kim, M. Mitomo, Relationship between microstructure and fracture toughness of toughened silicon carbide ceramics, Journal of the American Ceramic Society 84 (2001) 1347–1353.
[9] F. Rodríguez-Rojas, A.L. Ortiz, F. Guiberteau, M. Nygren, Oxidation behaviour of pressureless liquid-phase-sintered α-SiC with additions of

$5Al_2O_3 + 3RE_2O_3$ (RE = La, Nd, Y, Er, Tm, or Yb), Journal of the European Ceramic Society 30 (2010) 3209–3217.

[10] F. Rodríguez-Rojas, A.L. Ortiz, F. Guiberteau, M. Nygren, Anomalous oxidation behaviour of pressureless liquid-phase-sintered SiC, Journal of the European Ceramic Society 31 (2011) 2393–2400.

[11] O. Borrero-López, A.L. Ortiz, A. Pajares, F. Guiberteau, Hardness degradation in liquid-phase-sintered SiC with prolonged sintering, Journal of the European Ceramic Society 27 (2007) 3359–3364.

[12] O. Borrero-López, A.L. Ortiz, F. Guiberteau, N.P. Padture, Effect of microstructure on sliding-wear properties of liquid-phase-sintered α-SiC, Journal of the American Ceramic Society 88 (2005) 2159–2163.

[13] O. Borrero-López, A.L. Ortiz, F. Guiberteau, N.P. Padture, Microstructural design of sliding-wear-resistant liquid-phase-sintered SiC: an overview, Journal of the European Ceramic Society 27 (2007) 3351–3357.

[14] A.L. Ortiz, O. Borrero-López, M.Z. Quadir, F. Guiberteau, A route for the pressureless liquid-phase sintering of SiC with low additive content for improved sliding-wear resistance, Journal of the European Ceramic Society 32 (2012) 965–973.

[15] D.J. Green, An Introduction to the Mechanical Properties of Ceramics, Cambridge University Press, Cambridge, UK, 1998.

[16] G.R. Anstis, P. Chantikul, D.B. Marshall, B.R. Lawn, A critical evaluation of indentation techniques for measuring fracture toughness: I. Direct crack measurements, Journal of the American Ceramic Society 64 (1981) 533–538.

[17] B.R. Lawn, Indentation of ceramics with spheres: a century after Hertz, Journal of the American Ceramic Society 81 (1998) 1977–1994.

[18] N.P. Padture, Hertzian contacts, in: R.W. Cahn, K.H.J. Buschow, M.C. Flemings, B. Ilschner, E. Kramer, S. Mahajan, P. Veyssièr (Eds.), Encyclopaedia of Materials: Science and Technology, Pergamon Press, New York, 2001, pp. 3750–3752.

[19] H. Xu, T. Bhatia, S.A. Deshpande, N.P. Padture, A.L. Ortiz, F.L. Cumbrera, Microstructural evolution in liquid-phase-sintered SiC: I. Effect of starting SiC powder, Journal of the American Ceramic Society 84 (2001) 1578–1584.

[20] L.S. Sigl, H.-J. Kleebe, Core/rim structure of liquid-phase-sintered silicon carbide, Journal of the American Ceramic Society 76 (1993) 773–776.

[21] V.V. Pujar, R.P. Jensen, N.P. Padture, Densification of liquid-phase-sintered SiC, Journal of Materials Science Letters 19 (2000) 1011–1014.

[22] N.P. Padture, B.R. Lawn, Toughness properties of a silicon carbide with *in situ*-induced heterogeneous grain structure, Journal of the American Ceramic Society 77 (1994) 2518–2522.

[23] B.R. Lawn, N.P. Padture, L.M. Braun, S.J. Bennison, Model for toughness curves in two-phase ceramics. 1. Basic fracture-mechanics, Journal of the American Ceramic Society 76 (1993) 2235–2240.

[24] S.-J. Cho, B.J. Hockey, B.R. Lawn, S.J. Bennison, Grain-size and *R*-curve effects in the abrasive wear of alumina, Journal of the American Ceramic Society 72 (1989) 1249–1252.

[25] A.G. Evans, D.B. Marshall, Wear mechanism in ceramics, in: D.A. Rigney (Ed.), Fundamentals of Friction and Wear of Materials, American Society for Metals, 1981, pp. 441–452.